

Relayed FSO Links for Ground-to-Train Communications

N. Mohan¹, Z. Ghassemlooy¹, S. Zvanovec², M. Mansour Abadi¹, R. Hudson³ and M. R. Bhatnagar⁴

¹Optical Communications Research Group, Faculty of Engineering and Environment, Northumbria University, Newcastle upon Tyne, UK

²Department of Electromagnetic Field, Faculty of Electrical Engineering, Czech Technical University in Prague, Czech Republic

³The Core, Bath Lane, Newcastle Helix, Newcastle upon Tyne

⁴Department of Electrical Engineering, Indian Institute of Technology Delhi, New Delhi 110016, India

Abstract— *Pervasive use of smart phones and computing devices has led to an increase in network bandwidth demand on trains. Free space optics (FSO) is considered as one of the alternatives to provide high speed internet services on-board high-speed trains (HST). Due to frequent handovers both in the network and physical layers the user's experience is greatly affected. Relay assisted FSO, which is primarily used as a fading mitigation technique, can be employed to reduce the impact of network layer handover in the context of HST communications. In this paper, we propose a relay-based FSO system to provide ground to train communications and relays the information to the next base stations. Two schemes are analyzed via numerical simulations namely (i) all optical amplify and forward (AOAF); and (ii) AOAF with optical and optical-electronical-optical regeneration schemes in terms of the bit error rate performance and transmission range attained.*

Keywords— Free space optics, Relayed free space optics.

I. INTRODUCTION

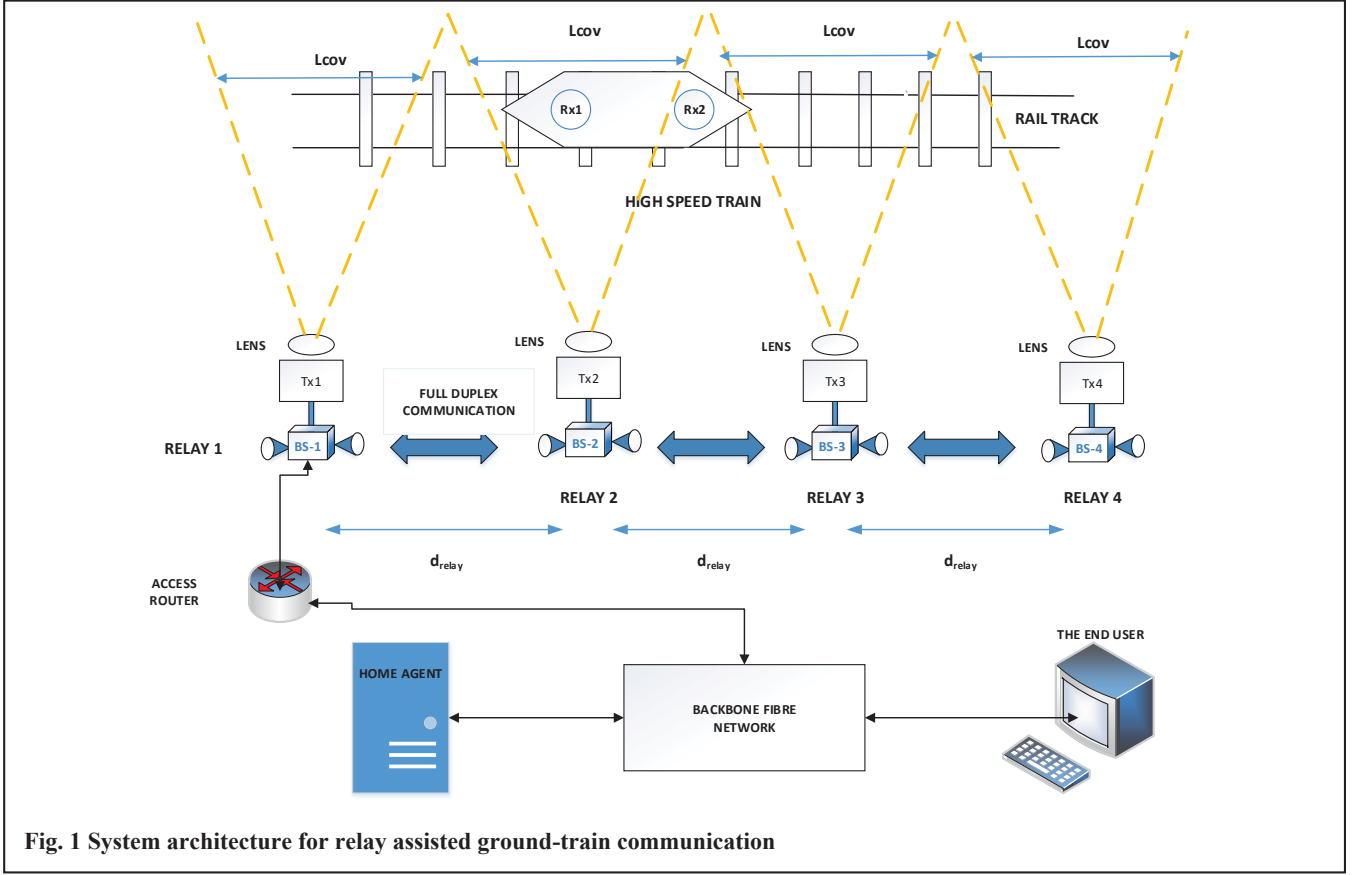
Development of a high-speed railway network such as High Speed 2 in the UK aims to connect the country and is expected to ferry around 300,000 passengers per day [1]. The ubiquitous use of hand-held devices such as smart-phones and laptops would lead to increased demand in the network bandwidth on board high-speed trains (HSTs). Providing high-speed internet in HSTs comes with many challenges. (i) Frequent handovers due to high-speed of trains, which will result in the degradation of quality of service (QoS) for passengers [2]. (ii) The implementation overhead required to execute the handover as trains leave the coverage area of one base station (BS) and approach the next BS. It is clear from above that, minimising the interruption time due to the handover process would improve the QoS requirement. Researchers in the past have proposed a system based on Wi-Fi [3] with an average handover time of 110 ms at train speeds of 270 km/hr. In [4], a mobile hot-spot network (MHN) was designed for subway trains using the millimetre-wave (mmW) technology with a carrier frequency of 25.5 GHz. The practical demonstration of MHN system yielded a 1.25 Gbps throughput for the downlink and 110 Mbps for the uplink [4]. In [5], a throughput of 1.5 Gbps using a 97 GHz mmW radio access system connected to a bidirectional radio over fibre (RoF) network for a train at a speed of up to 240 km/h was experimentally demonstrated. The mmW distributed radio access units deployed on the ground were connected to the bidirectional analogue RoF network for establishing a high-speed link with the on-board transceiver. In [6], a 20 Gbps wavelength division multiplexed fibre-radio frequency wireless

system at 90 GHz between the central station and the BS was investigated within an indoor environment. The work in [6] a high-speed moving-backhaul network using a switched wavelength division multiplexing (WDM) fiber-wireless system in the mmWave band was developed based on the moving BS concept where the HST communicates with the same BS in order to prevent frequent handovers. A high data rate (1 Gbps) ground to train communication (GTC) was proposed in [7], where an acquisition, tracking and pointing (ATP) mechanism based on the beaconing system was used to provide stable tracking and handover around 100 ms in FSO links for HST. In [8], a high-speed image sensor-based ATP mechanism was used in place of a 2-quadrant photodetector (PD) to detect the beacon signal from the adjacent BS. Using a new image processing algorithm for recognition and labelling beacon signals and a feedback control to control the direction of the mirror by employing a mirror angle sensor, the handover delay was reduced to 21 ms.

The network architecture for ground to train (G2T) communications consists of signal tapped from the backbone network via an access router (AR) serving a group of BSs on the ground connected to it. When a train passes from a BS to a successive BS connected to a different AR the transceiver on the train via a mobile router (MR) on board tries to establish a connection with the successive BS, which is termed as the link-layer handover. Note, MR sends a router solicitation message to the BS and the BS returns a router advertisement message to the MR, which signifies a successful link layer (L2) handover. The MR also sends a binding update message to the home agent, which in turn returns a binding acknowledgement message signifying the network layer (L3) handover at which point communications between the train and ground BS becomes available [7].

To mitigate L3 handover, this paper proposes a relayed FSO system, which enables G2T communications and relays the same data to successive BSs. Two schemes are considered and analyzed via numerical simulations which are all-optical amplify and forward (AOAF) and optical-electronical-optical regenerate and forward (OEORF) scheme in terms of the bit error rate (BER) performance and communication distance attained.

The rest of the paper is organised as follows. Section II describes the concept of relayed FSO for HST communications, Section III explains the signal model in the context of BS-BS



communications and section IV discusses the numerical results obtained for AOAF and OEORF.

II. RELAYED FSO FOR HST COMMUNICATIONS

A. System Architecture

The system architecture of the proposed link is described in Fig. 1, which comprises of a BS with a transceiver laser as a transmitter (Tx) and a relay node positioned along the rail trackside for a full duplex communications. Two receivers (Rxs) are mounted on the roof of the train to provide seamless connectivity. The BSs, which are placed 210 m apart as the coverage area L_{cov} for each BS is 210 m, transmit the received signal from the relays to the train [9]. The Tx₁ is connected to an AR connected to the backbone fibre network. The laser is connected to the MR is installed on the train. The MR registers the home network prefix and care of address (CoA) with the home agent, which is connected to the backbone fibre network.

III. SIGNAL MODEL

In the context of BS to BS communications, the received signal is given as:

$$y(t) = h(t) * x(t) + n(t), \quad (1)$$

where x is the transmitted signal, n is additive white Gaussian noise with variance σ_n^2 , $*$ is the convolution symbol and h is the channel gain, which is given by:

$$h = h_a h_t, \quad (2)$$

where h_a and h_t are the attenuation constants due to the atmospheric channel and turbulence, respectively. For a FSO link, h_a is given by Beer's law as [10]:

$$h_a = e^{-\beta l}, \quad (3)$$

where l is the link length in m and β is the attenuation coefficient in m^{-1} . The optical intensity I of a wave propagating in a turbulence channel undergoes random fading effect with the normalized variance or the scintillation index given as [11]:

$$\sigma_I^2 = \frac{\langle I^2 \rangle - \langle I \rangle^2}{\langle I \rangle^2}, \quad (5)$$

where $\langle \cdot \rangle$ denotes the ensemble average equivalent to long-time averaging with the assumption of an ergodic process. Based on (5), the strength of turbulence can be classified as weak ($\sigma_I^2 < 1$), moderate ($\sigma_I^2 \cong 1$) and strong ($\sigma_I^2 > 1$) [12].

Assuming plane wave propagation, σ_I^2 is given by [13]:

$$\sigma_I^2(D) = \exp \left[\frac{0.49 \sigma_R^2}{\left(1 + 0.653d^2 + 1.11\sigma_R^{\frac{12}{5}}\right)^{\frac{7}{6}}} + \frac{0.51 \sigma_R^2 \left(1 + 0.69 \sigma_R^{\frac{12}{5}}\right)^{-\frac{5}{6}}}{\left(1 + 0.9d^2 + 0.621 d^2 \sigma_R^2\right)^{\frac{12}{5}}} \right] - 1, \quad (6)$$

where $d = \frac{D}{2} \sqrt{\frac{k}{l}}$ is the circular aperture scaled by Fresnel zone provided, k is the wavenumber and D is the Rx's aperture diameter. σ_R^2 is Rytov variance given by:

$$\sigma_R^2 = 1.23 C_n^2 k^{7/6} l^{11/6}, \quad (7)$$

where C_n^2 is the refractive index structure parameter with typical values of $10^{-17} \text{ m}^{-2/3}$ and $10^{-13} \text{ m}^{-2/3}$ for weak and strong turbulence regimes, respectively [11].

For weak turbulence, the turbulence induced fading gain is given as [14]:

$$h_t = e^{\chi + iS}, \quad (8)$$

where, S is the phase and χ is the fading log-amplitude is normally distributed with mean μ and variance σ_χ^2 .

A. Power Budget Analysis

The received power can be expressed as a function of the transmit power P_{tx} and the system losses, which is given by:

$$P_{rx}(l) = 10^{\frac{(L_{atm}l)}{10}} \times 10^{\frac{(L_{misc})}{10}} P_{tx}, \quad (9)$$

where l is the link length and L_{atm} is given by [15]:

$$L_{atm} \text{ (dB/km)} = \frac{17}{V} \left(\frac{\lambda}{550} \right)^{-q}, \quad (10)$$

where V is the meteorological visibility in km, λ is the wavelength in nm and q is the size distribution of scattering particles, which follows Kruse [16] model and is expressed as:

$$q = \begin{cases} 1.6 & V > 50 \text{ km} \\ 1.3 & 6 \text{ km} < V < 50 \text{ km} \\ 0.16V + 34 & 1 \text{ km} < V < 6 \text{ km} \\ V - 0.5 & 0.5 & 1 \text{ km} < V < 1 \text{ km} \\ 0 & V < 0.5 \text{ km} \end{cases} \quad (11)$$

Note, L_{misc} is the losses due the Tx and the Rx optics, which is, in this case, assumed to be 2 dB. It is assumed that, for BS-to-BS communications the optical beam is collimated for which the geometric loss is not considered in (8).

B. AOAF Scheme

Consider an AOAF system as depicted in Fig. 2 where an optical amplifier (Erbium doped fibre amplifier, EDFA) at each BS re-amplifies and re-transmits the received signal from the previous BS to the next BS. The received signal at each BS is given as:

$$x_r^k(t) = h x_t^{k-1}(t) + n_b^k(t), \quad (12)$$

where $x_r^k(t)$ is the received signal at the k th BS, x_t^{k-1} is the transmitted signal at $(k-1)$ th BS and n_b^k is the background noise. Transmitted signal from the k th relay is given by:

$$x_t^k(t) = \sqrt{G_k} x_r^k(t) + n_{ASE}^k(t), \quad (13)$$

where, G_k is the amplifier gain, n_{ASE}^k amplified spontaneous emission (ASE) noise. Assuming that the signal, background noise, ASE noise and fading are all independent, the average optical signal to noise ratio (SNR) at the $(M+1)$ th BS is given by [17]:

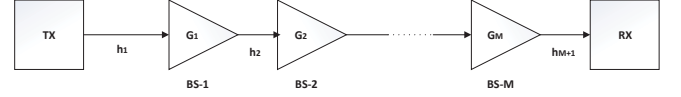


Fig. 2 The amplify and forward (AF) scheme

$$\text{SNR}^{M+1} = \frac{(\prod_{k=1}^M G_k h_k) h_{M+1} P_t}{(1 + \sum_{i=1}^M \prod_{k=i}^M G_k h_{k+1}) P_b + (h_{M+1} P_{ASE}^M + \sum_{i=1}^{M-1} \prod_{k=i+1}^M G_k h_k h_{M+1} P_{ASE}^i)} \quad (14)$$

where, P_t is average transmit power from the BS, P_b is background radiation power, P_{ASE}^j is ASE noise for the j th amplifier at that BS. The background radiation can be computed as [14]:

$$\sigma_{bg}^2 = \frac{N_0}{2}, \quad (15)$$

where, N_0 is the noise power spectral density.

C. Optical 2R Regenerator

With reference to Fig. 3, the degraded optical pulse from a relay is fed to an EDFA, which amplifies the signal to a suitable level at the input of a highly non-linear fibre (HNLF). The amplified pulse is launched into HNLF where the pulse experiences spectral broadening due to SPM (self-phase modulation). A narrow-band optical band-pass filter (OBPF) is used as a pulse shaping element to carve out the desired signal at the output.

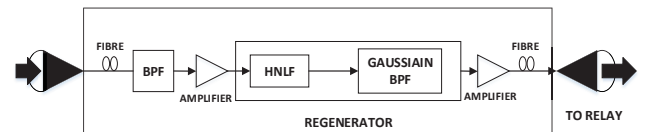


Fig. 3 Mamyshev 2R regenerator

The spectral broadening is given by [18]:

$$\Delta\omega_{SPM} = \Delta\omega_0 \left(\frac{2\pi}{\lambda} \right) n_2 I_p L, \quad (16)$$

where, $\Delta\omega_0$ is the initial bandwidth of the signal pulse, λ is the wavelength, n_2 and L are the refractive index and the length of the HNLF, respectively and I_p is the optical intensity of the pulse. Given that, the OBPF has a bandwidth of ω_f and is shifted by $\Delta\omega_{shift}$, the critical pulse intensity is given by [18]:

$$I_{cr} = \frac{2\Delta\omega_{shift}}{\Delta\omega_0 \left(\frac{2\pi}{\lambda} \right) n_2 L}. \quad (17)$$

From (11), the extent of spectral broadening can be controlled and from (12), the minimum input pulse intensity can be calculated. Please note that, the SPM based 2R regenerator is compatible for the return to zero (RZ) modulation format and preferred due to its simple implementation. For the OOK-RZ data format the BER is given as [19]:

$$\text{BER}_{\text{RZ-OOK}} = \frac{1}{2} \text{erfc}\left(\frac{\sqrt{\text{SNR}}}{2}\right). \quad (18)$$

D. OEO Regenerator

Fig. 4 provides a schematic diagram of a OEO-based repeater with forward error correction (FEC) coding. The received optical signal is converted to an electrical signal using a PD followed by a clock recovery (for obtaining the timing information from the signal) and a decoder module. The decoder counts the parity bits from the decoder to monitor performance. The FEC block performs error correction on the signal prior to being used for intensity modulation of the laser source via the current driver module [20]. This configuration is typically used at the client side. With respect to G2T communications this schematic can be used as the Rxs located on the train.

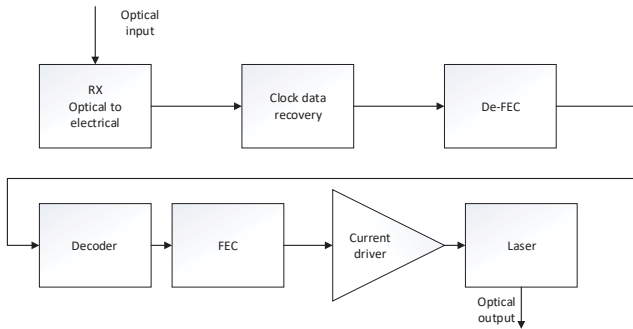


Fig. 4 OEO for FEC implementation.

IV. RESULTS AND DISCUSSION

In this section numerical simulation has been performed to evaluate the performance of amplify and forward (AF) relaying system and AF with the combination of 2R regenerator and an OEO regenerator. In all cases, the data rate considered is 10 Gbps with RZ-OOK, $\lambda = 1550$ nm, L_{atm} is -17.5 dB/km with a visibility of 800 m and the inter relaying distance is 210 m [9]. The average transmit power P_{tx} is estimated from (9). The noise contribution from the background radiation is assessed from (15) and the amplifier noise contribution is estimated from the noise figure given in Table 1. Since the relaying distance is less than 1 km long, Rytov variance from (7) is 0.114 for $C_n^2 = 1 \times 10^{-13} \text{ m}^{-2/3}$, which falls under the weak turbulence regime therefore not considered in this work. For optical regenerating relays a bandpass filter with 80 GHz followed by HNLFF with an attenuation of 0.88 dB/km and length of 500 m is considered. The optical bandpass filter has a central wavelength of 1551 nm and a bandwidth of 3 nm [18]. For OEO regenerators Reed-Solomon FEC (RS(255,233)) is considered for its low latency, low complexity and low power consumption [21].

A. AOAF with Relay

Consider an AOAF, where the communication distance attained from Fig. 5 is 1022 m within the FEC limit of 2.2×10^{-3} . The gross communications distance for the stations-to-BS is taken as 840 m, which is 4 hops as the 5th hop's is above the FEC limit.

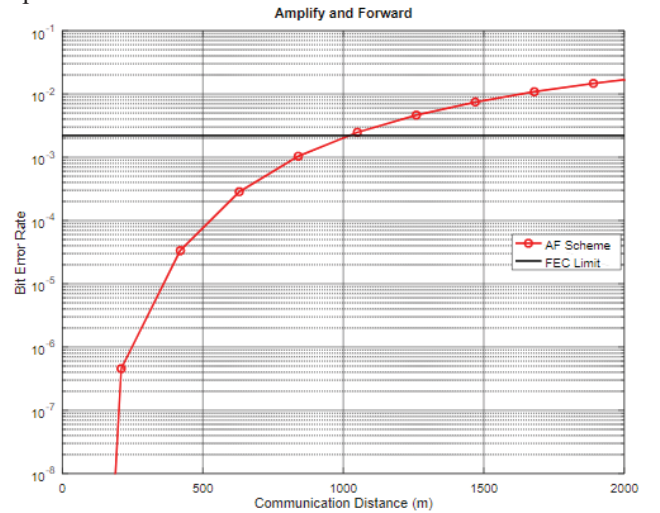


Fig. 5 The BER as function of the transmission distance for the AF relaying for stations-to-BS communications.

Accumulation of the background noise in the AF scheme limits the transmission range in BS-to-BS links. Note, for the 5th BS, the signal will need to be tapped from the backbone network via an AR. This would result in both the network and physical layers handover for the train passing from the 4th to the 5th BS.

TABLE 1 KEY SYSTEM PARAMETERS

SYSTEM PARAMETERS	
PARAMETER	VALUE
Operating wavelength	1550 nm
Train speed	300 km/hr
Photodetector type	PIN
Rx Wavelength range	500-1630 nm
Rx 3 dB bandwidth	10 kHz – 12 GHz
Noise equivalent power	24 pW/√Hz
Responsivity of PD at 1550 nm	0.85 A/W
P_{tx}	18.3 mW
EDFA	
Operating wavelength	1528-1564 nm
Output power	18 dBm to 26dBm
Noise figure	< 5 dB
Input power	-12 dBm to +7dBm
Laser class	3B

B. OEORF scheme

Consider an optical AF scheme with a 2R regenerator situated at the 3rd BS and with the OEO located at the 6th BS. The 2R regenerator placed in the 3rd BS will extend the link span from 4 hops (840 m) to 6 hops (1260 m) as shown in Fig. 6.

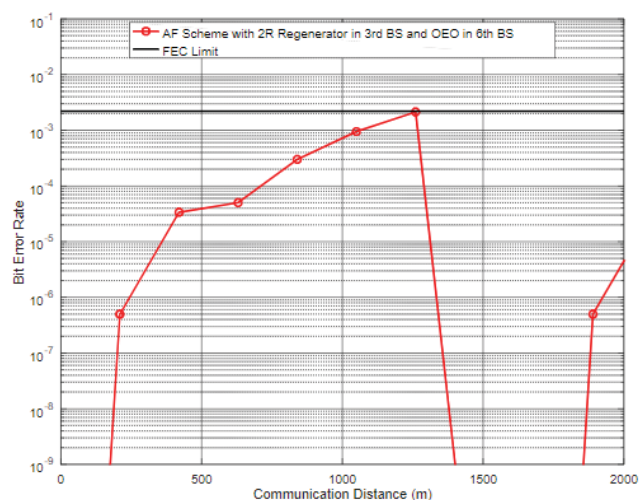


Fig. 6 The BER vs. transmission distance for the AF scheme with 2R regenerator at 3rd BS and OEO at 6th BS.

The OEO at the 6th BS employs error correction, thus resetting in error free transmission as in [22], which is then amplified and forwarded to the next BS. As compared with the AF scheme, the AF in tandem with the 2R regenerator and OEO requires no new AR to be installed as the scheme is contiguous, practically eliminating network layer handover.

CONCLUSION

This paper utilised the concept of relayed free space optics in the context of base station to base station communication in train to ground communications to mitigate network layer handover. Two schemes were analysed in the presence of atmospheric attenuation (17 dB/km) namely AOAF and OEORF. The total communication distance attained by AOAF is 840 m due to noise accumulation at each hop which results in signal tapped from the backbone network via an access router causing network handover delay along with physical layer handover delay. OEORF scheme provides contiguous communication distance without having to install any new access routers eliminating network handover delay.

ACKNOWLEDGMENT

This work is supported by intensive industrial innovation program northeast, United Kingdom (IIP NE) - 25R17P01847 and is partly funded by the European regional development fund (ERDF).

REFERENCES

[1] "What is HS2 | High Speed 2", High Speed 2, 2020. [Online]. Available: <https://www.hs2.org.uk/what-is-hs2/>. [Accessed: 15- Feb- 2020].

[2] L. Tian, J. Li, Y. Huang, J. Shi and J. Zhou, "Seamless Dual-Link Handover Scheme in Broadband Wireless Communication Systems for High-Speed Rail," in *IEEE Journal on Selected Areas in Communications*, vol. 30, no. 4, pp. 708-718, May 2012. doi: 10.1109/JSAC.2012.120505.

[3] K. Yamada, Y. Sakai, T. Suzuki, Y. Kawahara, T. Asami and H. Aida, "A Communication System with a Fast Handover under a High Speed Mobile Environment," 2010 IEEE 72nd Vehicular Technology Conference - Fall, Ottawa, ON, 2010, pp. 1-5. doi: 10.1109/VETEFC.2010.5594584.

[4] H. Chung et al., "From architecture to field trial: A millimeter wave based MHN system for HST Communications toward 5G," 2017 European Conference on Networks and Communications (EuCNC), Oulu, 2017, pp. 1-5.

[5] A. Kanno et al., "Field Trial of 1.5-Gbps 97-GHz Train Communication System Based on Linear Cell Radio Over Fiber Network for 240-km/h High-Speed Train," 2019 Optical Fiber Communications Conference and Exhibition (OFC), San Diego, CA, USA, 2019, pp. 1-3.

[6] P. T. Dat, A. Kanno, K. Inagaki, F. Rottenberg, N. Yamamoto and T. Kawanishi, "High-Speed and Uninterrupted Communication for High-Speed Trains by Ultrafast WDM Fiber-Wireless Backhaul System," in *Journal of Lightwave Technology*, vol. 37, no. 1, pp. 205-217, 1 Jan.1, 2019

[7] H. Urabe et al., "High Data Rate Ground-to-Train FreeSpace Optical Communication System," *Optical Engineering, Special Section on Free-Space Laser Communications*, vol. 51, no. 3, Mar. 2012.

[8] K. Mori et al., "Fast handover mechanism for high data rate ground-to-train free-space optical communication system," 2014 IEEE Globecom Workshops (GC Wkshps), Austin, TX, 2014, pp. 499-504.

[9] N. Mohan, M. Abadi, Z. Ghassemlooy, S. Zvanovec, R. Hudson and M. Bhatnagar, "Sectorised base stations for FSO ground-to-train communications," *IET Optoelectronics*, p. 8, 2020. Available: 10.1049/iet-opt.2019.0155 in press.

[10] E. Leitgeb, S. S. Muhammad, C. Chlestil, M. Gebhart and U. Birnbacher, "Reliability of FSO links in next generation optical networks," *Proceedings of 2005 7th International Conference Transparent Optical Networks*, 2005., Barcelona, Catalonia, 2005, pp. 394-401 Vol. 1

[11] S. Rajbhandari, Z. Ghassemlooy, P. A. Haigh, T. Kanesan and X. Tang, "Experimental Error Performance of Modulation Schemes Under a Controlled Laboratory Turbulence FSO Channel," in *Journal of Lightwave Technology*, vol. 33, no. 1, pp. 244-250, 1 Jan.1, 2015.

[12] M. M. Abadi, Z. Ghassemlooy, N. Mohan, S. Zvanovec, M. R. Bhatnagar and R. Hudson, "Implementation and Evaluation of a Gigabit Ethernet FSO Link for 'The Last Metre and Last Mile Access Network'," 2019 IEEE International Conference on Communications Workshops (ICC Workshops), Shanghai, China, 2019, pp. 1-6.

[13] M. A. Khalighi, N. Aitamer, N. Schwartz and S. Bourennane, "Turbulence mitigation by aperture averaging in wireless optical systems," 2009 10th International Conference on Telecommunications, Zagreb, 2009, pp. 59-66.

[14] S. Kazemlou, S. Hranilovic and S. Kumar, "All-Optical Multihop Free-Space Optical Communication Systems," in *Journal of Lightwave Technology*, vol. 29, no. 18, pp. 2663-2669, Sept.15, 2011.

[15] S. Fathi-Kazerooni et al., "Optimal Positioning of Ground Base Stations in Free-Space Optical Communications for High-Speed Trains," in *IEEE Transactions on Intelligent Transportation Systems*, vol. 19, no. 6, pp. 1940-1949, June 2018.

[16] P. W. Kruse, L. D. McGlauchlin, and R. B. McQuistan, *Elements of Infrared Technology: Generation, Transmission, and Detection*. New York, NY, USA: Wiley, 1962

[17] S. Kazemlou, "All-Optical Multihop Free-Space Optical Communication Systems", PhD, McMaster University, 2010.

- [18] N. Nor, M. Komanec, J. Bohata, Z. Ghassemlooy, M. Bhatnagar and S. Zvánovec, "Experimental all-optical relay-assisted FSO link with regeneration and forward scheme for ultra-short pulse transmission", *Optics Express*, vol. 27, no. 16, p. 22127, 2019.
- [19] T. Y. Elganimi, "Studying the BER performance, power- and bandwidth- efficiency for FSO communication systems under various modulation schemes," 2013 IEEE Jordan Conference on Applied Electrical Engineering and Computing Technologies (AEECT), Amman, 2013, pp. 1-6.
- [20] Frankel M, Livas J, inventors; Ciena Corp, assignee. Simplified signal regenerator structure. United States patent application US 11/090,047. 2006 Jun 15.
- [21] *Ieee802.org*. 2020. [Online]. Available: http://www.ieee802.org/3/ca/public/meeting_archive/2017/03/vanveen_3ca_1a_0317.pdf. [Accessed: 26- Feb-2020].
- [22] Ciaramella E. Wavelength conversion and all-optical regeneration: achievements and open issues. *Journal of Lightwave Technology*. 2011 Nov 24;30(4):572-82.